Scientific Report No. 34

ON TWO STAGGERED, PARALLEL LOOP ANTENNAS

by

Ahmed S. Abulkassem and David C. Chang

June 1978

Department of Electrical Engineering
University of Colorado

TABLE OF CONTENTS

List of Figures

ON TWO STAGGERED, PARALLEL LOOP ANTENNAS

by

Ahmed S. Abulkassem and David C. Chang

1. Introduction

Loop antennas have long been considered as one of the basic antenna forms for probing, transmitting, as well as receiving radio signals. As a result of these many uses, the radiation characteristics of a single, thin-wire, circular loop antenna have been investigated extensively in the past, at low frequency, as a magnetic dipole [1-5], as well as at frequency high enough to produce resonances and antiresonances [6-10]. However, because of the complex geometry, mutual coupling of arrays consisting of parallel loop elements has seldom been analyzed, except in the case of coaxial loops. To the best of our knowledge, the work by Bhattacharya et al. [10] appears to be the first which treated the problem of two staggered loop antennas. However, the accuracy of their solution is somewhat in question because they ignored the off-diagonal terms in the mutual coupling matrices. Thus the purpose of this paper is to assess the error in their solution as well as to provide a computational scheme for the general case of two parallel, staggered loop antennas. A thorough understanding of such a problem is important, not only to the synthesis of antenna arrays consisting of circular loops, but also in understanding the performance of a single loop, both horizontal and vertical over a highly conducting earth via the concept of images. As mentioned in [10], the staggered configuration may also improve the tracking resolution in direction finding.

2. Formulation of the Integral Equations

Consider two thin-wire, circular loops of radii b and a wire radius a arranged parallel to each other in a staggered manner as shown in Fig. 1. The two loop planes are separated by a distance z_o and their axes are separated by a distance ρ_o. The loops are respectively driven by slice voltage generators of amplitudes V_1 and V_2 located on the loops at angles ψ_{s1} and ψ_{s2} with respect to the x-axis. The suppressed time factor is $\exp(-i\omega t)$ and the condition,

$$a \ll \lambda, \quad \rho_o, \quad z_o \quad \text{and} \quad a^2 \ll b^2 \tag{1}$$

where λ is the wavelength in air, is assumed. On the surface of the antennas we require the total tangential $\bar{E}$-field, $E_{\psi n}(\psi_n)$, $n = 1,2$ to satisfy the boundary condition that

$$E_{\psi m} = -V_m \, \delta(\psi - \psi_{sm})/b \qquad -\pi \leq \psi \leq \pi \tag{2}$$

$m = 1,2$ where $\delta(\psi)$ is the Dirac delta function. Furthermore, because thin-wire approximation in (1), the proximity effect around the wire inherited in the geometry of the two loops is negligible so that the current on each loop can be considered uniform around the wire. To formulate the required integral equations, use is made of the magnetic vector potential $\bar{A}$ due to an element of current of strength $I_m(\psi'_m)bd\psi'_m$ on one of the two loops. The electric field $d\bar{E}$ provided by such an element of current is given in function of $\bar{A}$ as:

$$d\bar{E} = -\frac{C}{i\omega\mu_o\varepsilon_o}\left[\nabla(\nabla\cdot\bar{A}) + k_o^2\bar{A}\right] \tag{3}$$

where

$$C = \mu_o b I(\psi'_m) d\psi'_m/4\pi \; . \tag{4}$$

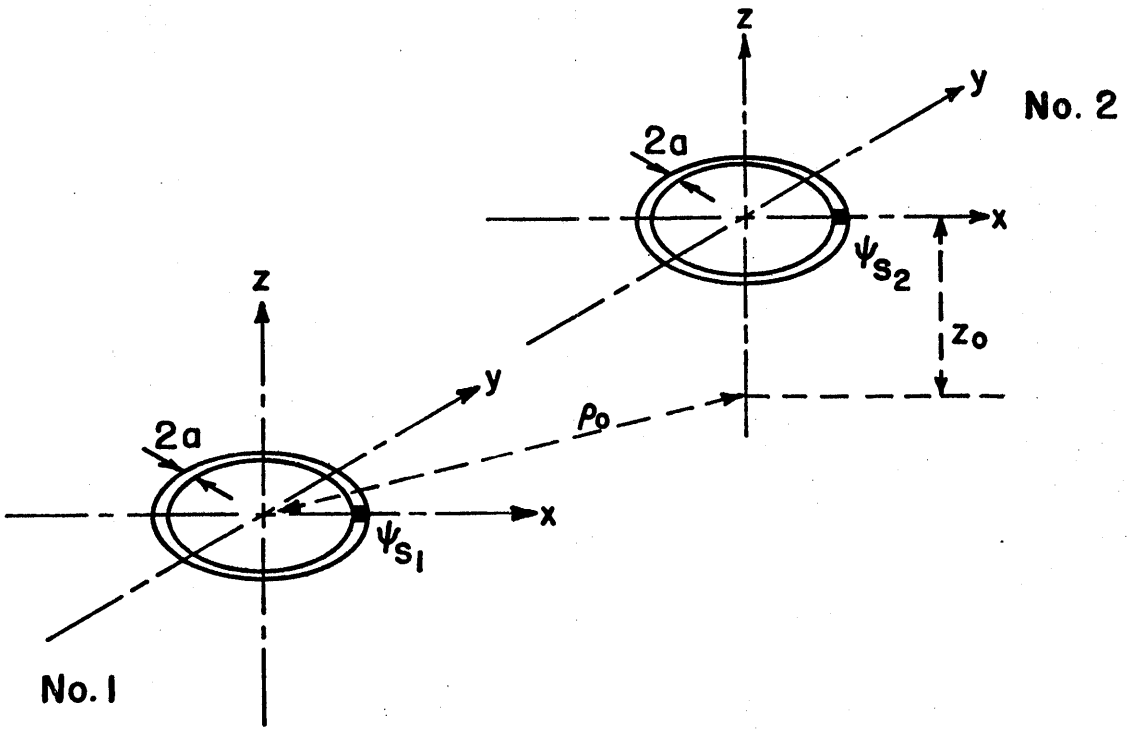

Fig. 1 Two staggered loop antennas

The total E-field contribution of all current elements of a loop is then obtained by integrating ψ' over the entire loop. To take the source singularity properly into account, the self-field of a loop is obtained from a current $I(\psi')$ distrubuted uniformly on the surface of the loop, even though the secondary field is obtained approximately from a line current located along the axis of the secondary loop. According to King [6] the primary vector potential $\bar{A}^P$ is then given by:

$$\bar{A}^P = G^P(\psi_m - \psi_m')[\bar{a}_{\psi'_m} \cdot \bar{a}_x)\bar{a}_x + (a_{\psi'_m} \bar{a}_y)\bar{a}_y] \tag{5}$$

where

$$G^P(\psi_m - \psi_m') = \frac{1}{2\pi}\int_{-\pi}^{\pi} \frac{e^{ik_o R(\psi_m - \psi_m')}}{k_o R(\psi_m - \psi_m')}\, d\phi \tag{6}$$

$$R(\psi_m - \psi_m') = [4b^2 \sin^2\left(\frac{\psi_m - \psi_m'}{2}\right) + 4a^2 \sin(\frac{\phi}{2})]^{\frac{1}{2}} \tag{7}$$

on loop $m = 1,2$. The ϕ-angle variation is around the thin wire of the loop. Similarly we obtain the expression for the secondary vector potential.

$$\bar{A}^S = G^S(\psi_m, \psi_n')[(\bar{a}_{\psi'_m} \cdot \bar{a}_x)\bar{a}_x + (\bar{a}_{\psi'_m} \cdot \bar{a}_y)\bar{a}y] \tag{8}$$

where

$$G^S(\psi_m, \psi_n') = e^{ik_o R(\psi_m, \psi_n')}/k_o R(\psi_m, \psi_n') \tag{9}$$

where

$$R(\psi_m, \psi_n') = [z_o^2 + (y_o + b \sin\psi_m - b \sin\psi_n')^2 + (x_o + b\cos\psi_n' - b\cos\psi_m)^2]^{\frac{1}{2}} \tag{10}$$

on loop m due to a current element on loop n. The geometry of the problem as projected in the plane perpendicular to the axes of the two loops is shown in Fig. 2 for clarity. To find the expression for the tangential component of the electric field on the two loops, one needs only to

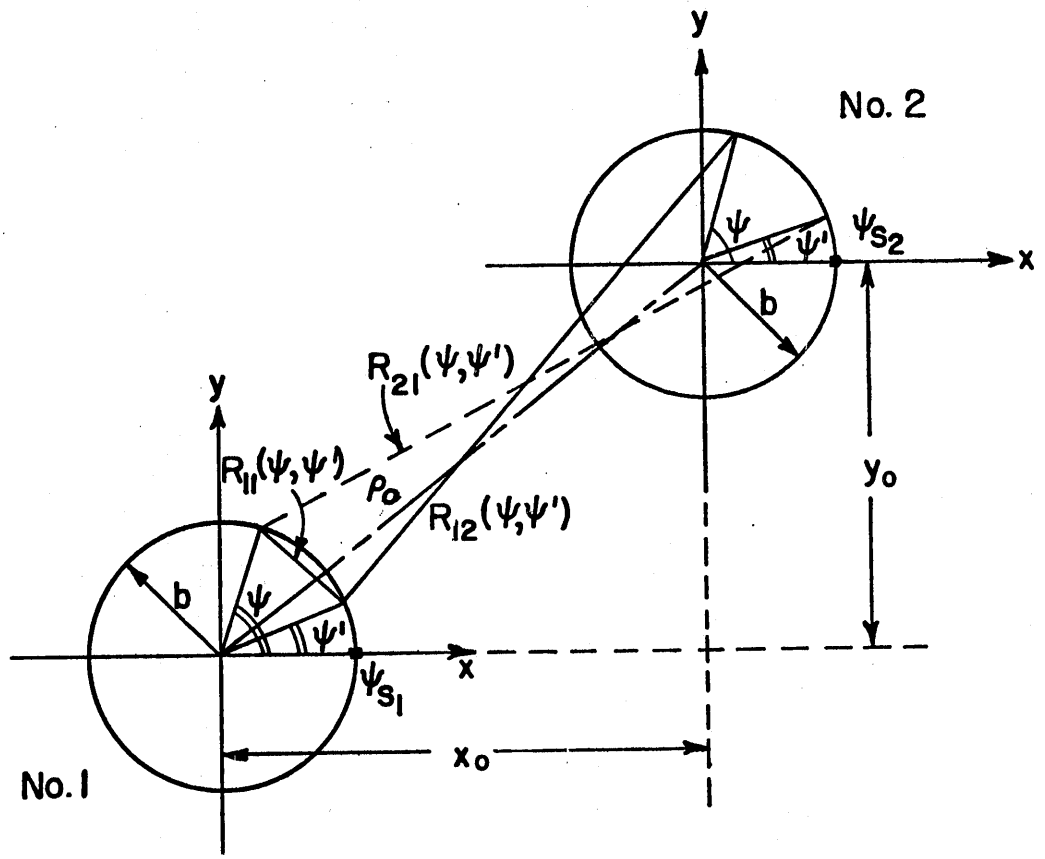

Fig. 2 Projection of the two staggered loops onto the horizontal plane perpendicular to their axes

evaluate $\bar{a}_\psi \cdot [\nabla(\nabla\cdot\bar{A}) + k^2\bar{A}]$. Now since $\nabla\cdot\bar{A} = -\nabla'\cdot\bar{A}$ the differential field at ψ on loop m due to a current element $I_m(\psi')bd\psi'$ on loop m and a current element $I_n(\psi')bd\psi'$ on loop n can be written as:

$$dE_{\psi_m} = \frac{i\omega d\psi'}{4\pi k_o b}\left\{\left(k_o^2 b^2 \cos(\psi-\psi') + \frac{\partial^2}{\partial\psi^2}\right)G_{mn}(\psi-\psi')I_m(\psi')\right.$$
$$\left. + \left(k_o^2 b^2 \cos(\psi-\psi') - \frac{\partial^2}{\partial\psi\partial\psi'}\right)G_{mn}(\psi-\psi')I_n(\psi')\right\} \tag{11}$$

where

$$G_{mm} = G^P(\psi_m - \psi_m'); \quad \text{and} \quad G_{mn} = G^S(\psi_m,\psi_n') \tag{12}$$

We now invoke the boundary condition $E_\psi = -V_m\delta(\psi-\psi_{s_m})/b$ on the surface of the two loops to obtain the following integral equations

$$\sum_{n=1}^{2} < Q_{mn}, \ I_n > = \frac{i4\pi}{\xi_o} V_m\delta(\psi-\psi_{s_m}) \tag{13}$$

for

$$-\pi \le \psi \le \pi, \qquad m = 1,2$$

where

$$Q_{mn} = [k_o^2 b^2 \cos(\psi-\psi') + \frac{\partial^2}{\partial\psi^2}]\ G_{mm}^P(\psi-\psi') \tag{14}$$

for m = n and

$$Q_{mn} = [k_o^2 b^2 \cos(\psi-\psi') - \frac{\partial^2}{\partial\psi\partial\psi'}]\ G_{mn}^S(\psi-\psi') \tag{15}$$

for $m \neq n$ $<\ >$ denotes the integration over the entire loop $-\pi \le \psi' \le \pi$; $\xi_o = 120\pi$ ohms is the characteristic impedance of free space. We note that since the two loops are parallel to each other, it is no longer necessary to distinguish ψ_1, ψ_1' from ψ_2, ψ_2' .

3. Solution of the Integral Equations Using Fourier Series

In order to solve the two simultaneous integral equations in (13) the current $I_m(\psi')$ is expanded in Fourier series as

$$I_m(\psi') = \sum_{q=-\infty}^{\infty} I_q^{(m)} e^{iq(\psi'-\psi_{sm})} \quad ; \quad m = 1,2 \tag{16}$$

where

$$I_q^{(m)} \, e^{-iq\psi_{sm}} = \frac{1}{2\pi} \int_{-\pi}^{\pi} I_m(\psi') e^{-iq\psi'} d\psi' \tag{17}$$

Similarly, the expansion of Green's function G_{mn} is given by

$$G_{mn}(\psi-\psi') = \sum_p K_p^p \; e^{ip(\psi-\psi')} \tag{18}$$

for $m = n$, and

$$G_{mn}(\psi,\psi') = \sum_p \sum_q (K_{pq}^s)_{mn} \; e^{ip\psi} \; e^{iq\psi'} \tag{19}$$

for $m \neq n$; and where

$$K_p^p = \frac{1}{2\pi} \int_{-\pi}^{\pi} e^{ip(\psi-\psi')} \; G_{mm}^p(\psi-\psi') d\psi' \tag{20}$$

and

$$(K_{pq}^s)_{mn} = \frac{1}{2\pi} \int_{-\pi}^{\pi} e^{ip\psi} \, d\psi \, \frac{1}{2\pi} \int_{-\pi}^{\pi} e^{-iq\psi'} \; G_{mn}^s(\psi,\psi') d\psi' \tag{21}$$

We note from the definition of G_{mn} as given in (12) and (8) that the following relationship holds.

$$(K_{pq}^s)_{nm} = (-1)^{(p+q)} \; (K_{pq}^s)_{mn} \tag{22}$$

So that one need not compute $(K_{pq}^s)_{21}$, once $(K_{pq}^s)_{12}$ is known, the substitution of (16), (18) and (19) into the integral equations (13) yields, after some manipulations,

$$\sum_p a_p^P I_p^{(1)} e^{ip(\psi-\psi_{s1})} + \sum_p \sum_q (a_{pq}^s)_{12} I_{-q}^{(2)} e^{i(p\psi+q\psi_{s2})}$$

$$= i \frac{2}{\xi_o} V_1 \delta(\psi-\psi_{s1}) \tag{23}$$

$$\sum_p \sum_q (a_{pq}^s)_{21} I_{-q}^{(1)} e^{i(p\psi+q\psi_{s1})} + \sum_p a_p^P I_p^{(2)} e^{ip(\psi-\psi_{s2})}$$

$$= \frac{i2}{\xi_o} V_2 \delta(\psi-\psi_{s2}) \tag{24}$$

where a_p^P and a_{pq}^s are the moment functions of the primary field component and the secondary field component respectively. They are given by:

$$a_p^P = (K_{p+1}^P + K_{p-1}^P) \frac{k_o^2 b^2}{2} - p^2 K_p^P \tag{25}$$

and

$$a_{pq}^s = (K_{p+1,q-1}^s + K_{p-1,q+1}^s) \frac{k_o^2 b^2}{2} + pq\, K_{pq}^s \tag{26}$$

where K_{pq}^s and a_{pq}^s are understood as $(K_{pq}^s)_{12}$ and $(a_{pq}^s)_{12}$; $(a_{pq}^s)_{21}$ are also given by (26) with their corresponding $(K_{pq}^s)_{21}$ related to $(K_{pq}^s)_{12}$ through equation (22).

Multiplying both sides of the above set of equations in (23) and (24) by $e^{-ip(\psi-\psi_{sm})}$, $m = 1,2$ and integrating over ψ, from $-\pi$ to $+\pi$, both sides of the two equations we obtain after some easy manipulations.

$$\sum_q [a_p^P I_q^{(1)} \delta_{pq} + (a_{pq}^s)_{12} I_{-q}^{(2)} e^{i(p\psi_{s1} + q\psi_{s2})}] = i V_1/\pi\xi_o$$

$$\sum_q [(a_{pq}^s)_{21} I_{-q}^{(1)} e^{i(q\psi_{s1} + p\psi_{s2})} + a_p^P I_q^2 \delta_{pq}] = iV_2/\pi\xi_o \tag{27}$$

for $p = 1,2, \ldots$ and $q = 1,2, \ldots$,

where δ_{pq} is the Kronecker delta, i.e. $\delta_{pq} = 1$ for $p = q$ and $\delta_{pq} = 0$

otherwise. Each of the above equations in (27) is an infinite system of linear equations. Expressions for the model currents $I_q^{(1)}$ and $I_q^{(2)}$ can now be obtained by truncation of the two sets of equations followed by an inversion of the related matrices.

4. Results and Discussion

It is clear from (27) that before the model currents are obtained it is necessary to compute the moment functions a_p^P and a_{pq}^s through (25) and (26) respectively after computing K_p^P and K_{pq}^s. Following the work by Wu [8,11], K_p^P are computed according to the following expression:

$$K_p^P = (4\pi kb)^{-1} \{K_o(p\tfrac{a}{b})\, I_o(p\tfrac{a}{b}) + C_p - (\pi/2)Q_o\}$$

where

$$C_p = \gamma - 2 \sum_{m'=0}^{p-1} (2m'+1) + \ell n(4p)$$

$$Q_o = \int_o^{2k_o b} [\Omega_{2p}(x) - iJ_{2p}(x)]dx$$

where Ω_p is the Lommel-Weber function defined as

$$\Omega_p(x) = \frac{1}{\pi}\int_o^{\pi} \sin(x \sin\theta - p\theta)d\theta ,$$

and J_p is the Bessel function of order p. $I_o(x)$ and $K_o(x)$ are modified Bessel functions of the first kind and the second kind respectively, and of order zero, and where $\gamma = 0.577216$ is the Euler's constant and a and b are the radius of the wire and the loop respectively. For more detail the reader is referred to the original work of Wu [8] or the review article by King [6].

On the other hand, K_{pq}^s are computed directly from (21) by numerically performing the double integration. A double Gaussian-Legendre quadrature is adopted so that (21) was transformed into a double summation of the form

$$(K_{pq}^s)_{mn} = \sum_{\alpha=1}^{N}\sum_{\beta=1}^{N} A_\alpha A_\beta\, G_{mn}^s(\psi_\alpha,\psi_\beta) e^{-ip\psi_\alpha} e^{-iq\psi_\beta} ,$$

(α, β are integers).

where N depends on the order of quadrature used. A_α, A_β are weighting functions and ψ_α and ψ_β are the roots of the corresponding Legendre polynomial. A computer program is developed to compute the moment functions in arrays $[Z_{pq}]_{mn}$, $m = 1,2$; $n = 1,2$. Here $[Z]_{11}$ and $[Z]_{22}$ are diagonal self-impedance matrices with the nonzero elements given by $Z_{pp} = a_p^p$ in (25); $[Z]_{12}$ and $[Z]_{21}$ are mutual impedance matrices with each element Z_{pq} given by (26). The column vectors $[I_q]_1$ and $[I_q]_2$ resulting from the inversion of the system of matrices in (27) are then used in (16) to obtain the current distributions on the loops. In addition, the input admittance of one of the two loops is simply given by

$$Y_{in,_m} = \frac{I_m(\psi)}{V_m}\bigg|_{\psi=\psi_{sm}} = \sum_p \frac{I_p^{(m)}}{V_m} \quad ; \quad m = 1,2 \tag{29}$$

We note at this stage that in the result given by Bhattacharyya, et al., [10] the off-diagonal terms in $[Z]_{12}$ and $[Z]_{21}$ which represent the mutual coupling of the $p^{\underline{th}}$ Fourier component on one loop to the $q^{\underline{th}}$ component on the other are totally ignored.

In order to check the validity of our results, a comparison is made between normalized power radiation (i.e. real part of y_{in}) of two electrically small coplanar loops, driven in phase, and two parrallel horizontal magnetic dipoles as obtained by Vogler and Noble [12] using the EMF method. The agreement, in this case, is shown in Table I, to be well within 0.1% even for reasonably large loops of radius $k_o b = 0.1$.

To study the effect of proximity on resonant loops, current distribution of two coplanar loops of radius $k_o b = 1$ and wire radius $k_o a = 0.0156$ or equivalently $\Omega = 2\ell n\,(2\pi b/a) = 12$, are shown in Fig. 3 and Fig. 4, for two different heights $d/\lambda = 0.17$ and $d/\lambda = 0.50$.

TABLE I

COMPARISON BETWEEN HORIZONTAL MAGNETIC DIPOLE ABOVE A PERFECT CONDUCTOR (VOGLER and NOBLE) AND TWO PARALLEL COPLANAR LOOPS WITH $k_o b = 0.1$ and $\Omega = 12$.

d/λ	Conductance		Resistance	
	unnormalized ($\mho$) G	normalized* G_n	unnormalized (Ω) R	normalized* R_n
0.2	8.8184×10^{-7} mho	1.	2.1775×10^{-2} ohm	1.
0.25	6.7797×10^{-7} mho	0.7688	1.6747×10^{-2} ohm	0.7691
0.3	5.5739×10^{-7} mho	0.6321	1.3776×10^{-2} ohm	0.6327
0.35	5.3432×10^{-7} mho	0.6059	1.3209×10^{-2} phm	0.6066
0.4	5.9601×10^{-7} mho	0.6759	$1.4730 \times 10^{-]}$ ohm	0.6765
0.45	7.0874×10^{-7} mho	0.8037	1.7510×10^{-2} ohm	0.8041
0.5	8.2946×10^{-7} mho	0.9406	2.0486×10^{-2} ohm	0.9408

*Normalized G_n and normalized R_n are obtained by dividing their values at different heights to their value at $d/\lambda = 0.2$.

The voltage sources V_1 and V_2 are set at $\psi_{s_1} = -\pi/2$ and $\psi_{s_2} = \pi/2$ respectively for the case of Fig. 3 and at $\psi_{s_1} = \psi_{s_2} = 0$ for the case of Fig. 4. In each case, the proximity effect causes a decrease in current amplitude. A slight shift in the pattern is observed when the excitation is at $\psi_{s_1} = \psi_{s_2} = 0$. As expected, current distribution is symmetrical about $\psi = \pi/2$ in the case of Fig. 3.

The input admittance variation about its free space value is investigated as a function of loop separation for four different cases as shown in Figs. 5-8. The normalized distanced 2d is defined as the separation between the centers of the two loops with respect to free space wavelength. The first case is when the loops are coaxial; the second and third cases are for two staggered loops with inclination angle $\theta = 76°$ and $27°$ respectively. The fourth case is that of two coplanar loops ($\theta = 0°$). For the case when the excitations are located at $\psi_{s_1} = -\pi/2$ and $\psi_{s_2} = \pi/2$ Figs. 5 and 6 show that generally the coupling between the two loops decreases as the inclination angle θ decreases from a coaxial arrangement ($\theta = 90°$) to a coplanar one. The same behavior is shown in Fig. 7 and 8 when excitations are located at $\psi_{s_1} = \psi_{s_2} = 0°$. We notice in this case that the variation of G and B about their free space values is somewhat less pronounced. The curves with subscript $G_h(\theta = 0°)$ in Fig. 7 and $B_h(\theta = 0°)$ in Fig. 8 represent respectively the change in G and B in the case when the off diagonal terms were ignored [10]. The discrepancy between this case the the coplanar case is obviously very noticeable.

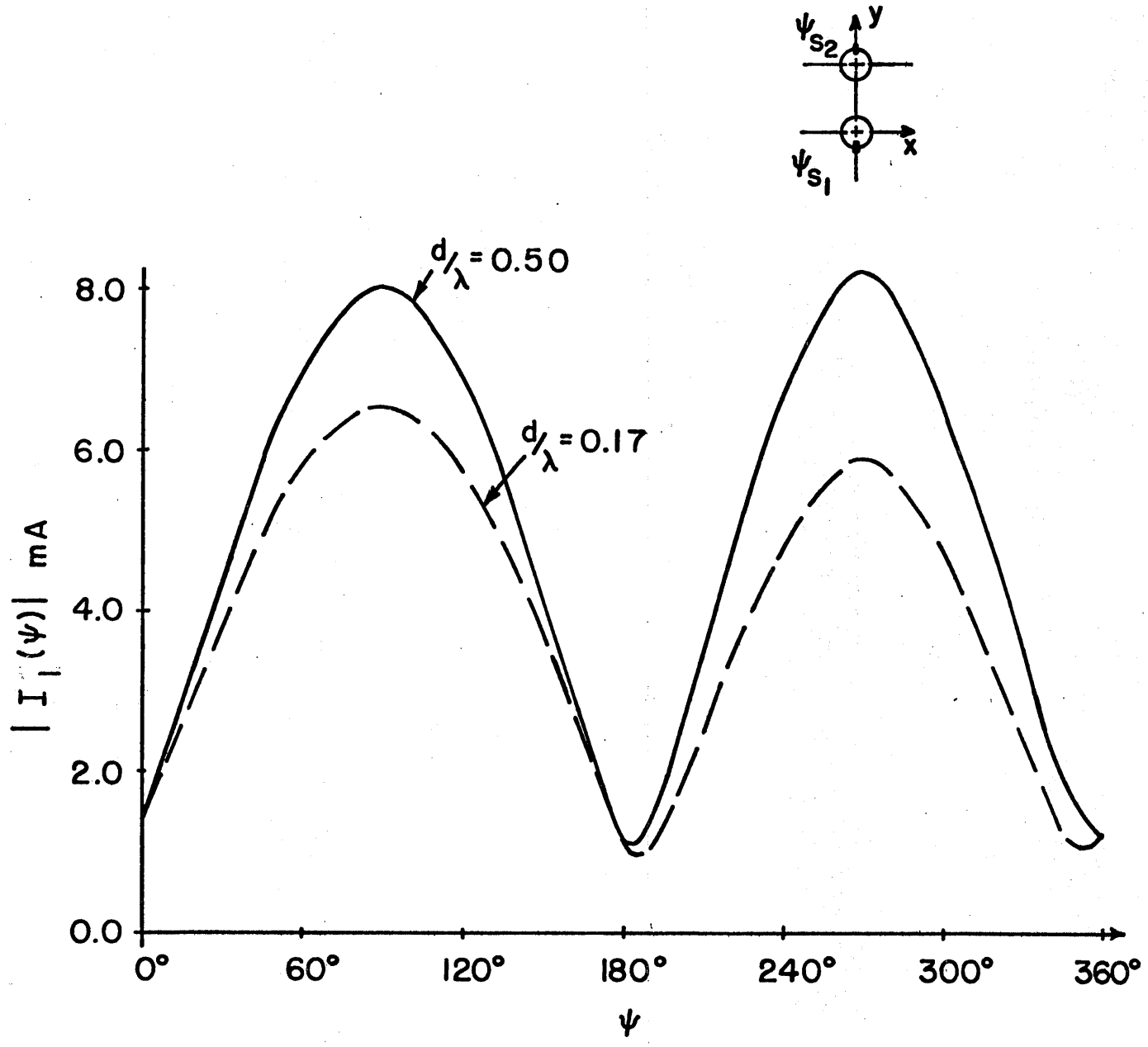

Fig. 3 Current distribution on loop 1 for $d/\lambda = 0.17$ and $d/\lambda = 0.50$ with sources located at $\psi_{s1} = -\pi/2$ and $\psi_{s2} = \pi/2$

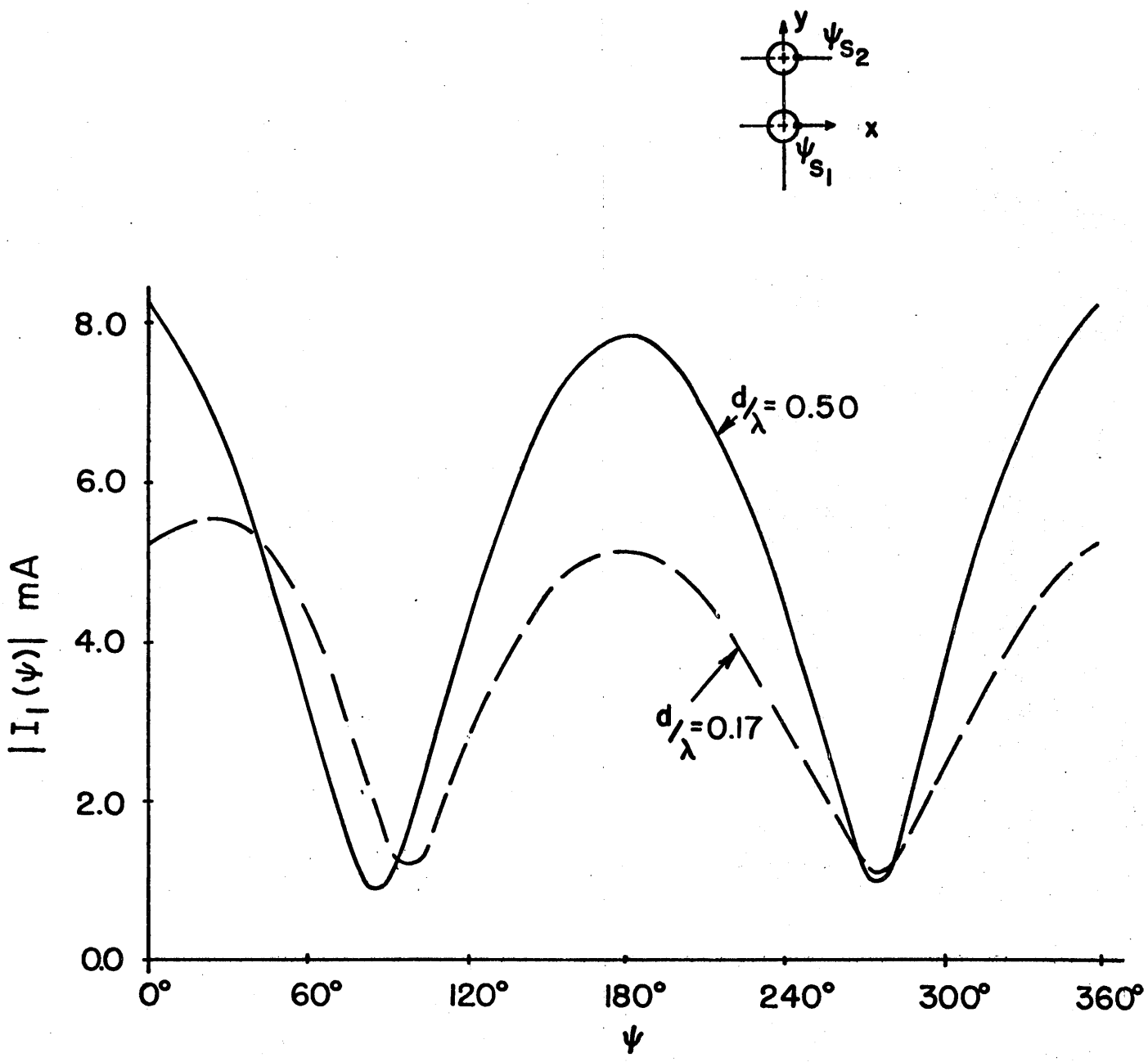

Fig. 4 Current distribution on loop 1 for $d/\lambda = 0.17$ and $d/\lambda = 0.50$ with sources located at $\psi_{s1} = \psi_{s2} = 0$

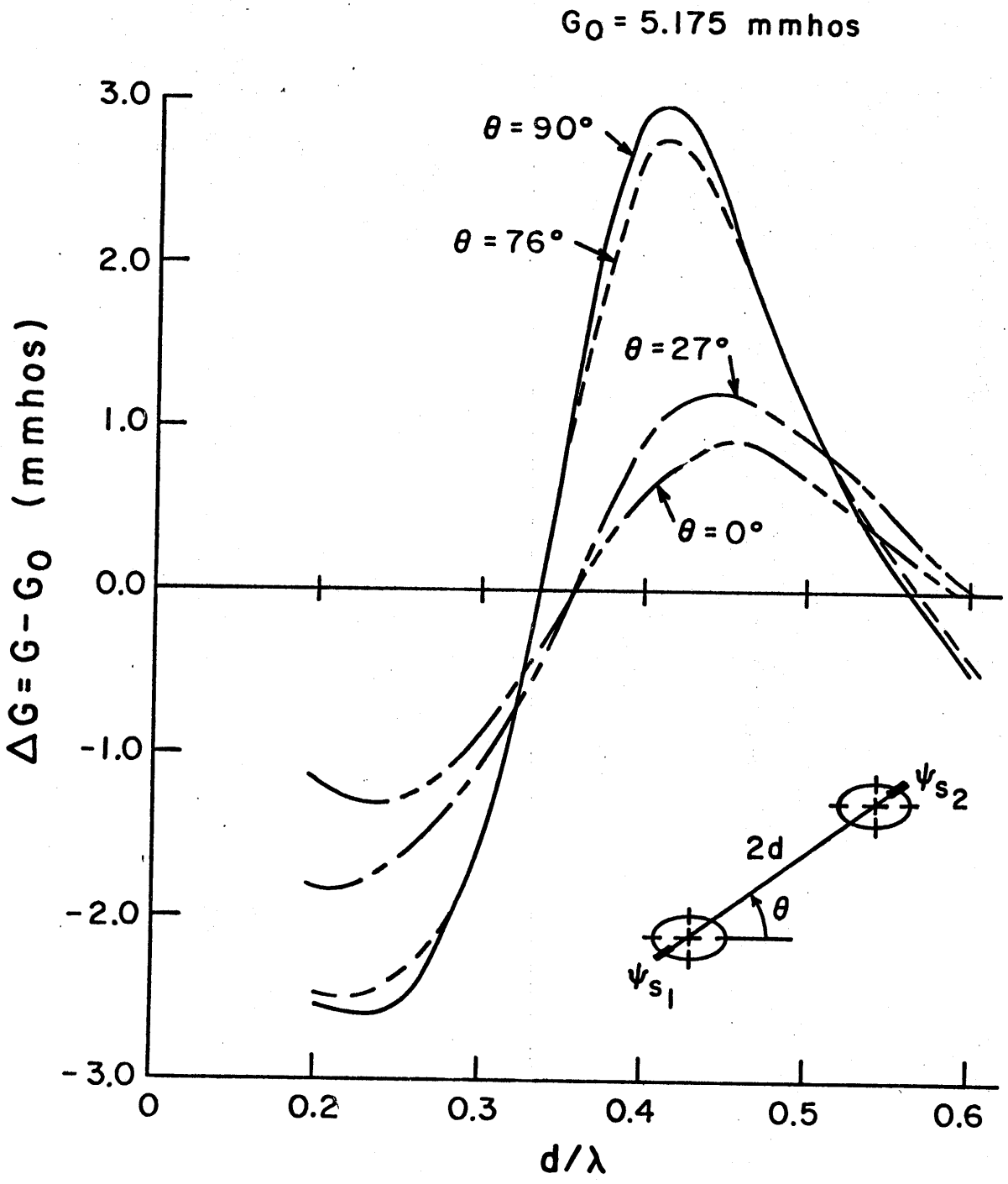

Fig. 5 Change in input conductance as a function of loop separation; sources are located at $\psi_{s1} = -\pi/2$ and $\psi_{s2} = \pi/2$

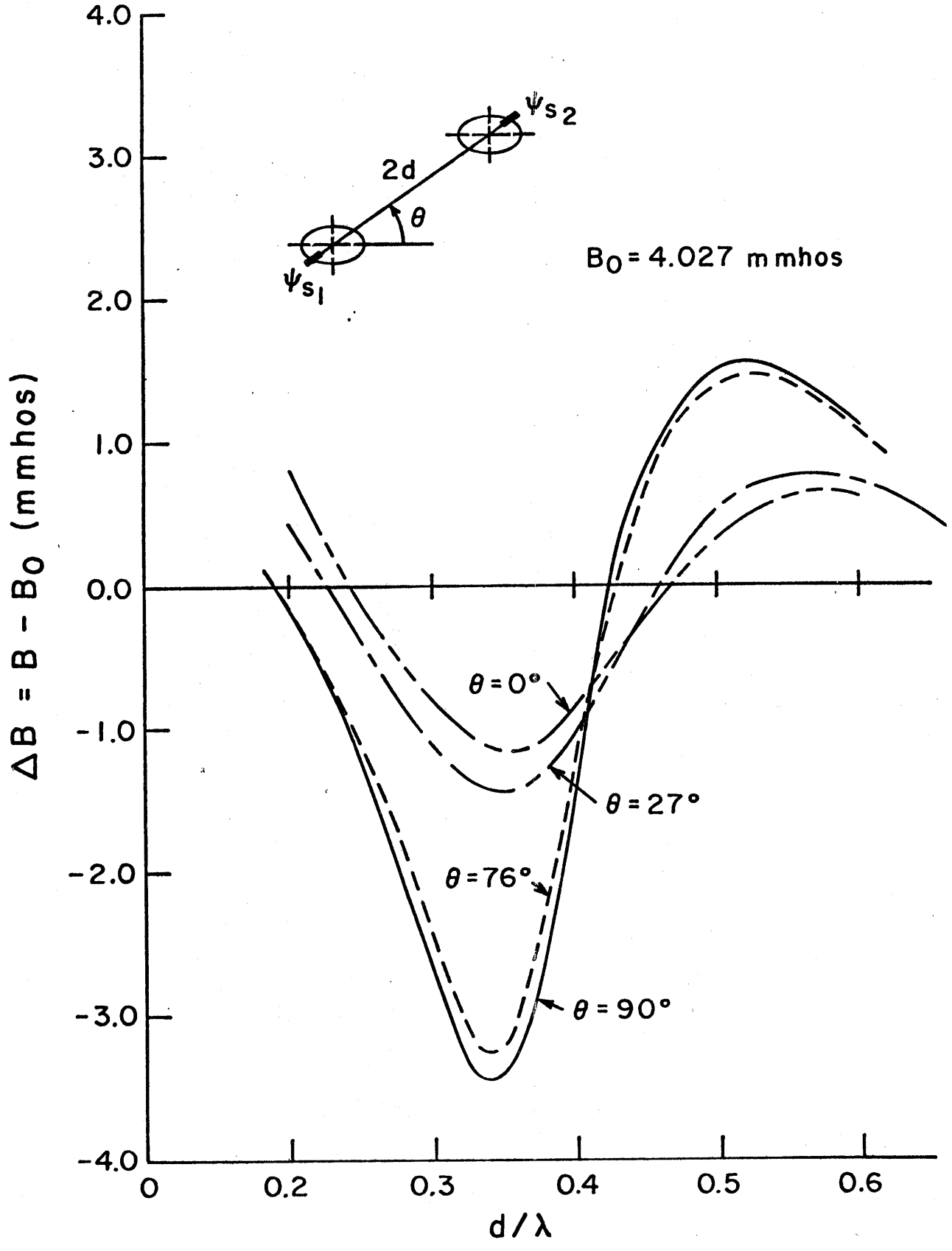

Fig. 6 Change in input susceptance for the two loops in Fig. 5

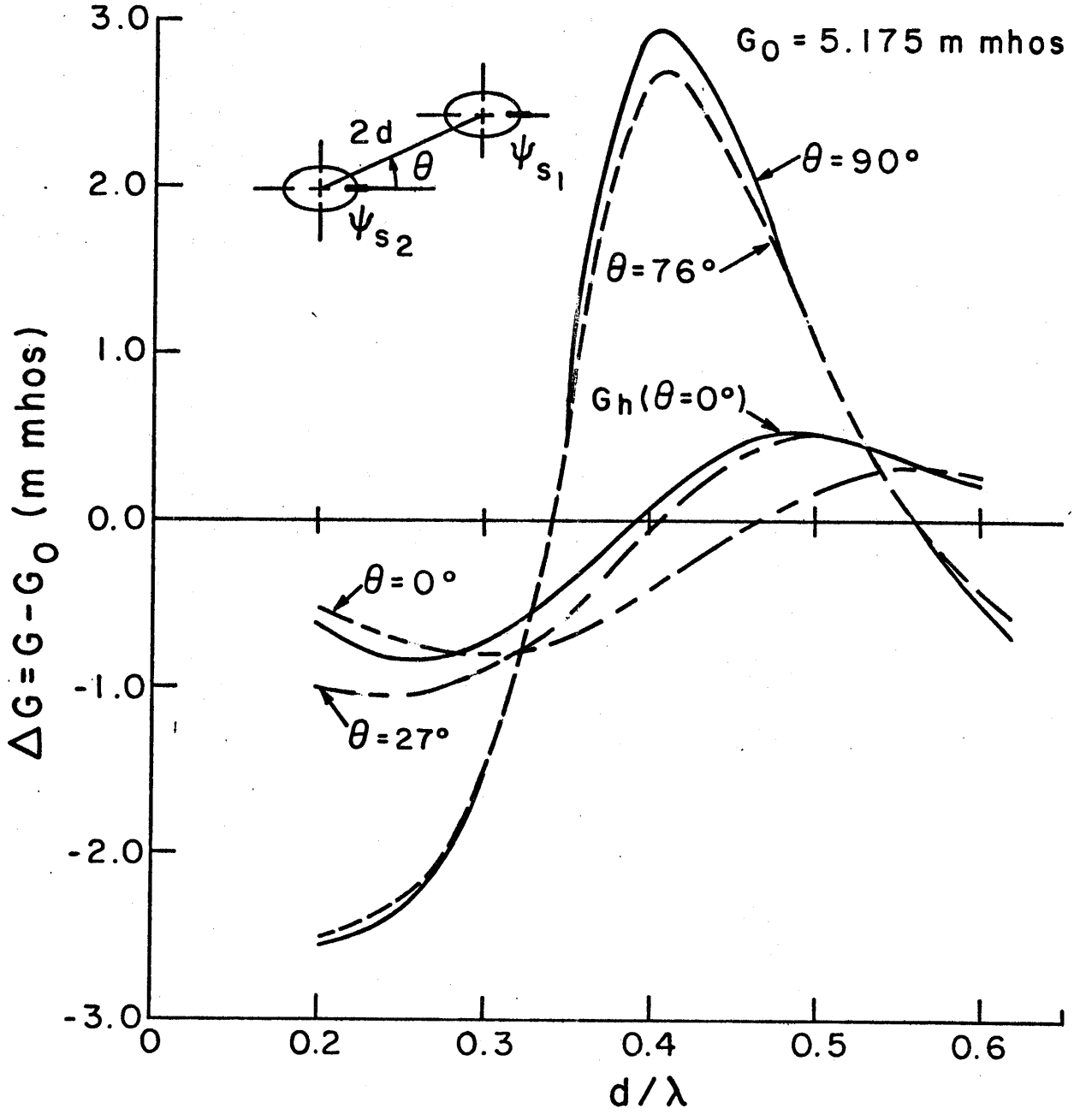

Fig. 7 Change in input conductance as function of loop separation; sources are located at $\psi_{s1} = \psi_{s2} = 0$

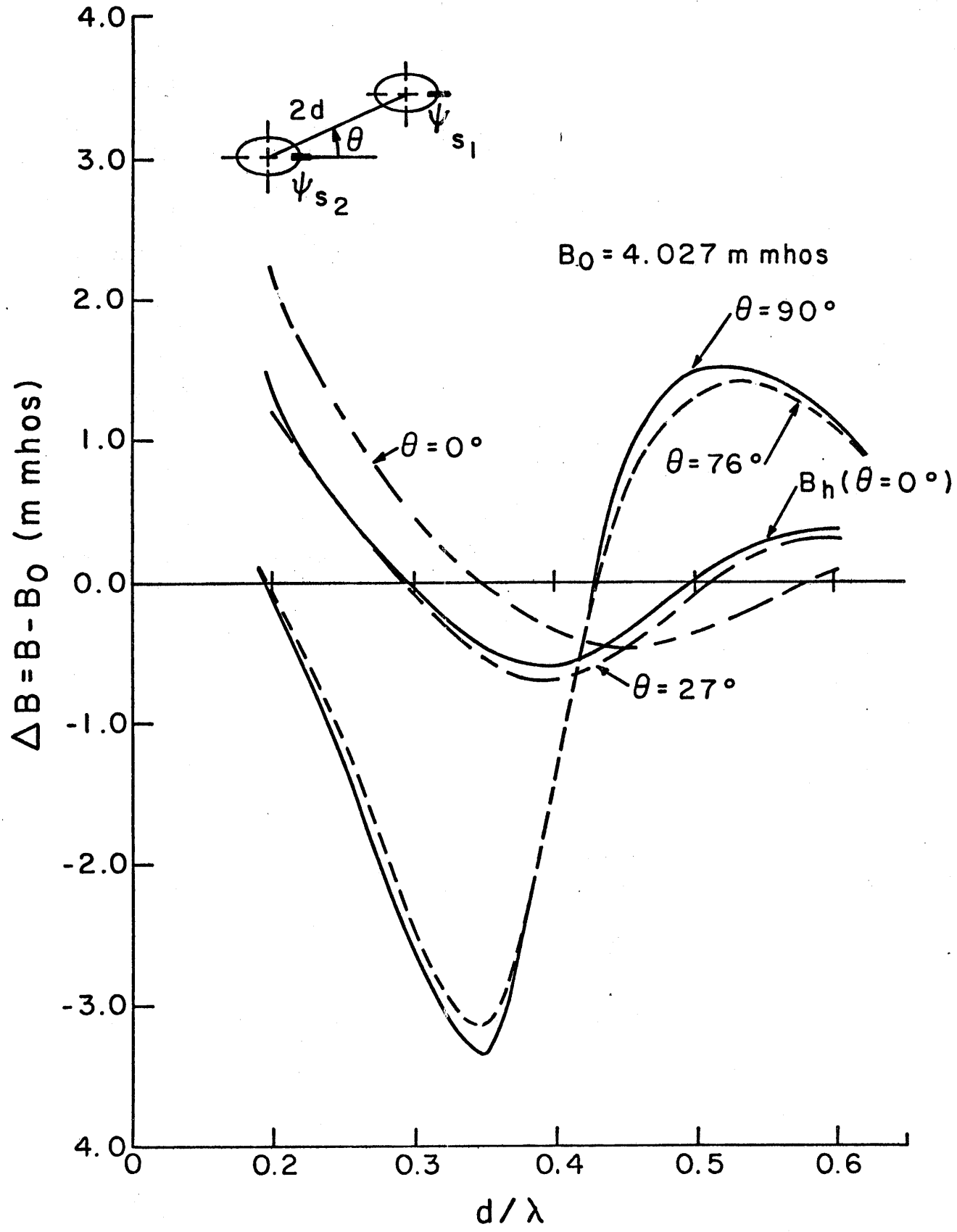

Fig. 8 Change in input susceptance for the two loops in Fig. 7

REFERENCES

[1] Baños, A. Jr. (1966), Dipole Radiation in the Presence of a Conducting Half Space, 1st ed., Pergamon Press, Oxford, England, Ch. 1 and 2, 1-63.

[2] Bhattacharyya, B.K. (1963), "Input resistance of a horizontal electric and vertical magnetic dipole over a homogeneous ground," IEEE Trans. Ant. and Prop., AP-11, No. 3, 261-266.

[3] A. Sommerfeld and F. Renner (1942), "Radiation energy and earth absorption for dipole antenna," Wireless Engineer, 19, No. 227, 351-359.

[4] Wait, J.R. (1953), "Radiation resistance of a small circular loop in the presence of a conducting ground," J. Appl. Phys., 24, 646-649.

[5] Wait, J.R. (1969), Characteristics of Antennas over Lossy Earth, Antenna theory (ed. Collin and Zucker), New York: McGraw-Hill, Pt. 2, Ch. 23, 386-437.

[6] King, R.W.P. (1969), Loop Antenna for Transmission and Reception, Antenna Theory (ed. Collin and Zucker), New York: McGraw-Hill, Pt. 1, Ch. 11, 458-482.

[7] King, R.W.P. and C.W. Harrison, Jr. (1969), Antenna and Waves, A Modern Approach, The M.I.T. Press, Ch. 9, 539-597.

[8] Wu, T,T, (1962),"Theory of thin circular antenna," J. Math. Phys. Vol. 3, 1301-1304, 1962.

[9] Slorer, J.E. (1956), "Impedance of thin wire antennas," Trans. AIEE, Vol. 75, 606-619.

[10] Bhattacharyaa, T. and Bandyopadhyay, K.K. (1973), "Analysis of element admittances of a pair of staggered loop antennas," Proc. IEE, Vol. 120, No. 12, 1482-1484.

[11] Chang, D.C. (1971), "Characteristics of a horizontal loop antenna over a dissipative half-space," Tech. Rept. No. 4, Dept. of Elec. Engr., University of Colorado, Boulder, CO.

[12] Vogler, L.E. and J.L. Noble (1964), "Curves of input impedance change due to ground for dipole antennas," NBS Monograph, No. 72, Dept. of Commerce, Boulder, CO.